

# Unexpected solids from enantiopure cationic palladium complexes and racemic anions: A structural study of chiral non-discrimination

Irmgard Kalf, Ruimin Wang, Ulli Englert\*

*RWTH Aachen University, Institute of Inorganic Chemistry, Landoltweg 1, 52074 Aachen, Germany*

Received 30 September 2005; received in revised form 9 November 2005; accepted 10 November 2005

Available online 20 December 2005

## Abstract

Enantiomerically pure cationic complexes were obtained via cyclopalladation of primary amines and subsequent addition of a chelating ethylenediamine ligand. No diastereomeric resolution was observed upon combining these cations with racemic mandelate or hydratropate anions, but four less popular products, namely three double salts and a solid solution, were obtained and structurally characterized. For one of the double salts, the alternative ionic compounds based on different stereoisomers of the same residues were synthesized independently: The conventional racemic solid and both diastereomeric salts formed by enantiopure cations and anions were studied by single crystal X-ray diffraction. Lattice energy calculations confirm that the diastereomeric salts differ significantly; formation of the partially racemic double salt, however, is energetically favourable and precludes resolution.

© 2005 Elsevier B.V. All rights reserved.

**Keywords:** Chirality; Resolution; Cyclopalladation; X-ray structure analysis; Lattice energy calculations

## 1. Introduction

For the separation of enantiomers the conversion of a racemate (*R*-I, *S*-I) to a mixture of diastereomers via treatment with one enantiomer of a chiral substance (e.g., *R*-II) represents the most popular method. Most frequently, the difference in solubility between diastereomeric salts has been exploited for resolution [1]. As early as 1910, Pope and Read [2] have classified attempted resolutions based on crystallization into three categories: (a) The diastereomeric salts (*R*-IR-II and *S*-IR-II) crystallize separately. This standard behaviour often permits efficient resolution, because one of these salts will be less soluble than the other and hence the one enantiomer of I involved in its formation will precipitate. (b) A stoichiometric “double salt” (*R*-IR-II)<sub>*n*</sub>(*S*-IR-II)<sub>*m*</sub> (*m*, *n* small integer numbers, frequently *m* = *n* = 1) can form, in which both enantiomers of the racemate targeted for resolution are present. This case

has been studied in detail almost a century ago by Ladenburg [3] who coined the term “partially racemic compound”. Neither the precipitate nor the solution will contain a pure enantiomer. (c) The enantiomers may be able to substitute each other in the crystal; consequently, the diastereomeric salts may form solid solutions of the type (*R*-I/*S*-I)*R*-II [4]. Structural studies devoted to the first category, i.e., to successful resolution via formation of diastereomers, have associated packing and intermolecular interactions, especially hydrogen bonding, to solubility or efficiency of resolution [5–12].

In this contribution, we wish to address the second and third case, in other words: the structural aspects of chiral non-resolution. Our examples comprise the structure of a solid solution and three double salts from the realm of organometallic chemistry; the four compounds result from combining related ionic constituents. Although double salts have been classified as “not exceptional” [13], structural studies are either rare or well hidden in the literature. We are aware of two reports on double salt structures, both dealing with organic compounds [14,15].

\* Corresponding author. Fax: +49 241 8092288.

E-mail address: [ullrich.englert@ac.rwth-aachen.de](mailto:ullrich.englert@ac.rwth-aachen.de) (U. Englert).

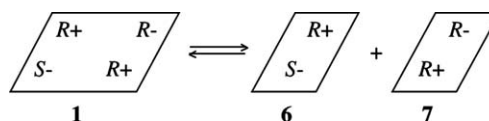
## 2. Results and discussion

In a systematic study on conglomerates and racemic crystals we are investigating ionic compounds of chiral organometallic complexes. In this context we synthesized the salts derived from racemic mandelic or hydratropic acid and two enantiomerically pure and structurally related cationic complexes. Contrary to our initial expectation, all four combinations resulted in solids containing both enantiomers of the anions, either in the form of double salts or as a solid solution. The compounds prepared and structurally characterized are compiled in [Scheme 1](#).

How do the partially racemic products **1–4** relate to the solids based on more conventional combinations of stereoisomers? Each double salt competes with a mixture of diastereomeric products; [Scheme 2](#) exemplifies this situation for the double salt **1** and the ionic compounds made up of enantiomerically pure constituents, namely **6** and **7**.

For this example of partially racemic **1** vs. enantiopure **6** and **7** we have performed a detailed structural study of the crystallization alternatives. In addition to the solids relevant for [Scheme 2](#), we have included the racemic compound **5** in our comparison which represents a yet different combination of stereoisomers of the same ionic residues.

First the four essential constituents of our structurally characterized compounds will be discussed. The palladium-organic cations were obtained according to [Scheme 1](#). The primary amines 1-phenylethylamine and 1-(4-methylphenyl)ethylamine were cyclopalladated and converted to chloro-bridged dinuclear complexes by well-established methods [16,17]. Related dinuclear compounds, mostly naphthyl rather than phenyl derivatives, have been used successfully for resolution via formation of diastereomers [18–21]. The chloro-bridged intermediates were cleaved by the silver carboxylates ([Scheme 1](#)) in the presence of ethylen-



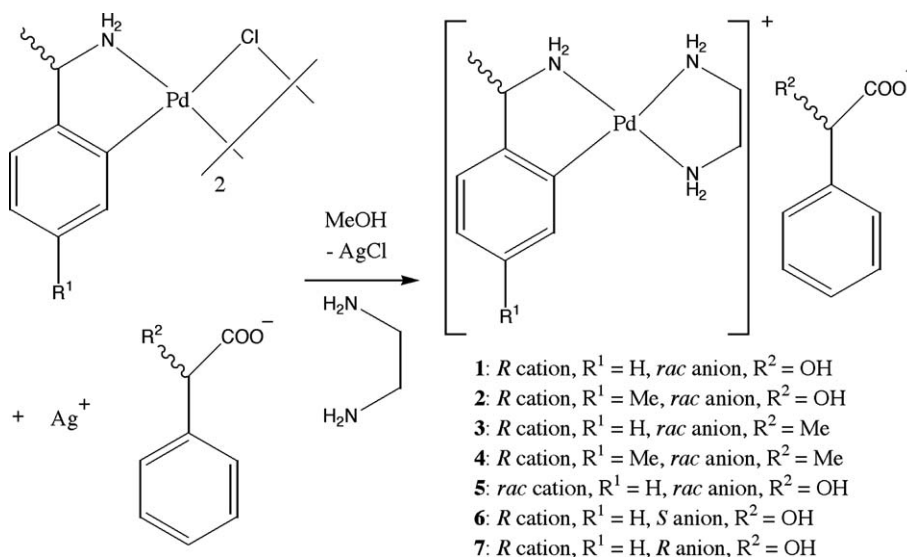
Scheme 2. Crystallization alternatives: Double salt precipitation (left) vs. formation of diastereomeric salts (right).

amine (en). We note that reaction of the dinuclear complexes with chelating ligands such as ethylenediamine or 2,2'-bipyridine in the absence of a suitable scavenger for the chloride in general results in equilibria between the starting material and the product, i.e., the chlorides of the cationic complexes. For ethylenediamine, this equilibrium lies on the product side. The obvious approach of introducing the counter anion in the form of a silver salt ensures quantitative conversion and allows for a variety of anions.

Most of the crystal structures described in this work contain two symmetrically independent cations and anions; in total eight cyclopalladation products of 1-phenylethylamine and four derivatives of the para methylated ligand have been characterized. Examples of displacement ellipsoid plots for these square-planar complex cations are shown in [Figs. 1 and 2](#), and palladium-ligand distances are compiled in [Table 1](#).

The bond lengths between the metal and the ethylenediamine nitrogen atoms differ significantly, the distance *trans* to Pd–C being on average 0.09 Å longer than the *cis* interaction. As expected, the cations are essentially flat; the dihedral angles subtended by the coordination plane (N1, N2, N3, C1) and the cyclopalladated six-membered aromatic ring range between 2.09(14)° and 17.20(18)°.

The carboxylate counteranions, with the exception of the two disordered hydratropate residues in the solid solution **4**, are conformationally similar. [Fig. 3](#) shows



Scheme 1. General reaction pathway and stereochemistry of the final products.

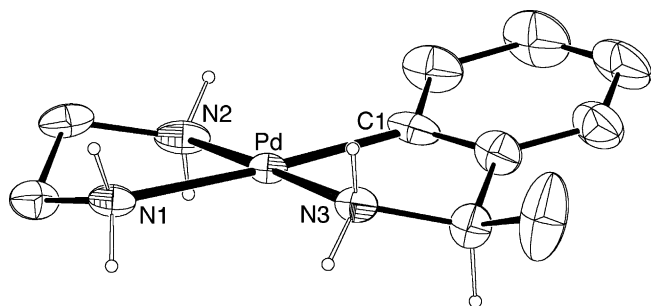


Fig. 1. Displacement ellipsoid plot (PLATON [22]) of one of the two symmetrically independent cations in **1**. Ellipsoids are scaled to 50% probability; only H atoms bonded to N or the chiral center are shown.

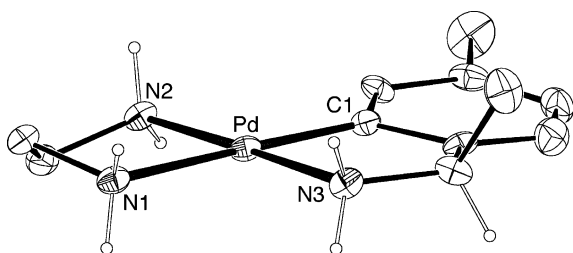


Fig. 2. Displacement ellipsoid plot (PLATON [22]) of one of the two symmetrically independent cations in **2**. Ellipsoids are scaled to 50% probability; only H atoms bonded to N or the chiral center are shown.

Table 1

Palladium–ligand distances (Å). Standard uncertainties are given in parentheses; for atom labels see Figs. 1 and 2

Compound		Pd–N1	Pd–N2	Pd–N3	Pd–C1
<b>1</b>	Molecule 1	2.127(9)	2.043(12)	2.055(10)	1.944(11)
	Molecule 2	2.166(10)	2.068(12)	2.039(11)	2.023(12)
<b>2</b>	Molecule 1	2.142(8)	2.048(8)	2.061(8)	1.963(19)
	Molecule 2	2.126(8)	2.066(8)	2.023(8)	1.995(10)
<b>3</b>	Molecule 1	2.155(4)	2.058(3)	2.046(3)	1.978(4)
	Molecule 2	2.157(4)	2.053(3)	2.048(3)	1.972(5)
<b>4</b>	Molecule 1	2.174(3)	2.058(2)	2.040(2)	1.974(3)
	Molecule 2	2.174(3)	2.059(2)	2.042(3)	1.982(3)
<b>5</b>		2.147(3)	2.051(3)	2.039(3)	1.972(3)
<b>6</b>	Molecule 1	2.168(9)	2.043(9)	2.041(9)	1.948(12)
	Molecule 2	2.120(10)	2.073(9)	2.038(9)	2.005(10)
<b>7</b>	Molecule 1	2.1494(16)	2.0658(16)	2.0399(14)	1.9810(16)
Average		2.150	2.057	2.043	1.978

the displacement ellipsoid plot for one of the eight symmetrically independent mandelate anions we encountered throughout this work. These hydroxycarboxylates adopt a conformation suitable for an intramolecular hydrogen bond which corresponds to a  $S_1^1(5)$  motif according to the graph set notation [23,24].

This structural feature favours coplanarity of the hydroxyl group with a carboxylate O atom; consequently, all torsion angles O3–C12–C11–O2 are found in the interval reported earlier by Larsen and De Diego [25]. Numerical values for this angle scatter around  $0^\circ$  (min.  $-4.9(13)$ ,

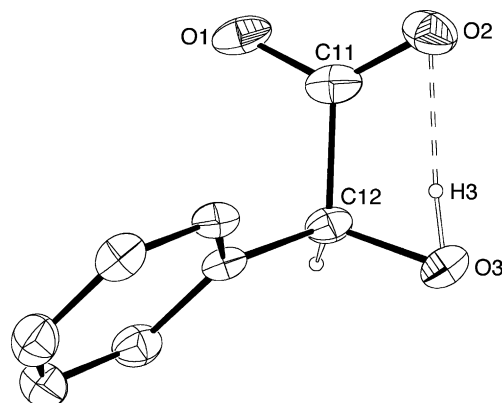


Fig. 3. Displacement ellipsoid plot (PLATON [22]) of the mandelate anion in **5**. Ellipsoids are scaled to 50% probability; only the hydroxyl H and the hydrogen atom bonded to the chiral center are shown.

max.  $2.6(12)$ ), with the only exception of a single relatively large angle of  $37.9(9)^\circ$  in one of the symmetrically independent anions of compound **6**. Without being enforced by intramolecular attractive interactions, the conformational similarity extends to the two well-defined hydratropate anions in  $3 \cdot \text{H}_2\text{O}$ .

We selected the ionic constituents described above because we expected that their close relationship with respect to size and conformation would allow to perceive structural trends and additional insight. In the following section we will focus on packing and intermolecular interactions. The crystal structures of the double salts **1–4** combine close space filling and efficient hydrogen bonding: packing coefficients lie between 0.696 and 0.714, and most of the potential hydrogen bond donors or acceptors find their partner at a reasonable distance. We note that this latter condition is not fulfilled in **7**, see below. Compounds **1** and **2** differ by just one substitution of a H atom by a methyl group in the cation; their structures are closely related. The difference in packing is reflected in significantly longer Pd···Pd distances of  $5.4 \text{ \AA}$  in **2** vs.  $4.5 \text{ \AA}$  in **1**.

It is understandable that intermolecular interactions change when we move from the mandelates **1** and **2** to the hydratropates **3** and **4**, i.e., when the hydroxyl group is replaced by methyl in the anions. One might expect, however, a certain structural similarity between the two hydratropate derivatives, comparable to the relationship between the two mandelates **1** and **2**. Although both **3** and **4** represent salts of the same anion and the only difference between the cations is due to the methyl substitution in the cations, entirely different structures arise. **3** was crystallized from methanol/water by evaporation and turned out to be a monohydrate and the only solvate in this study. Each water molecule acts as H bond donor towards two carboxylate anions and accepts hydrogen bonds from amino groups of two cations (Fig. 4).

Compound **4** was crystallized from acetonitrile; no attempt was made to exclude humidity, but in contrast to **3** no solvent molecules are incorporated into the crystal structure. The asymmetric unit contains two independent

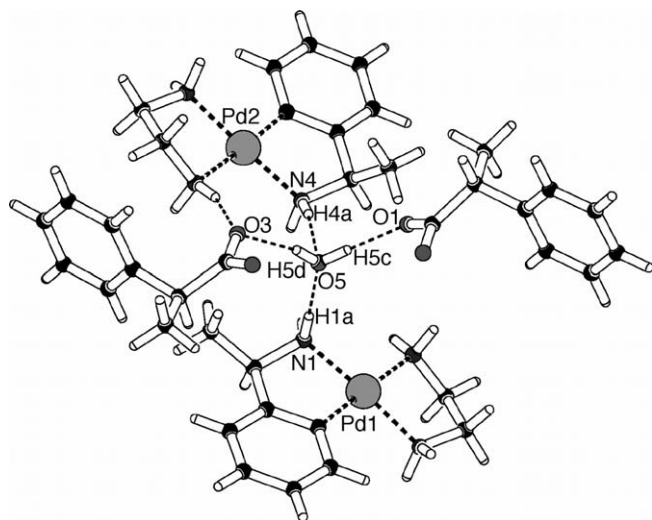


Fig. 4. Hydrogen bonding environment for one of the two symmetrically independent water molecules in the structure of **3** · H<sub>2</sub>O; the coordination of the second water molecule is similar. N–H bonds have been idealized to 0.92, O–H bonds to 0.85 Å. Hydrogen bond geometries: N1···O5 2.982(4) Å, N1–H1a···O5 179°; N4···O5 2.999(4) Å, N4–H4a···O5 165°; O5···O1 2.671(4) Å, O5–H5c···O1 179°; O5···O3 2.735(4) Å, O5–H5d···O3 165°.

cations of the same chirality (*R* configured in our example) and two anions which show disorder at their chiral centers. In the context of the present study, these disordered anions represent the only residues in which both *R* and *S* configuration coexist at the same crystallographic site.

We have reported the structures of the closely related double salts **1** and **2**, of the well-ordered solvate **3**, and of the solid solution **4**: All of them represent solids which are usually NOT considered when the readily available diastereomeric salts *R*-1*R*-2 and *S*-1*R*-2 are compared and discussed in order to explain successful resolution. At least one direct lesson can be learned from the mere existence of **1–4**: these less studied solids are probably more frequent than expected! Notably, mandelate, a common agent for diastereomeric resolution, has been involved in an earlier report of a double salt [14] and also represents one of the anionic residues in this work.

In order to learn more about the relative stabilities and the structural relationships between the partially racemic compounds and alternative crystallization products, we proceeded to synthesize and characterize all obvious [26] diastereomeric solids which are accessible when different enantiomers of the chiral ionic constituents of **1** are combined. The close similarity between the double salt **1**, the racemic compound **5**, and one of the diastereomeric salts, namely **6**, the product obtained from *R* configured cations and *S* mandelate anions, becomes obvious under various aspects: Tables 2 and 3 show that all three solids contain two cations and two anions per unit cell and have similar lattice parameters, belonging either to the triclinic space group *P*1 (**1** and **6**) or to its centrosymmetric supergroup *P*1̄ (**5**). Fig. 5 shows how pseudo-inversion relates the independent residues in **1** (Fig. 5(a)) and **6** (Fig. 5(c)) and provides a visual comparison of their packing similarities and differences with respect to racemic **5** (Fig. 5(b)).

Table 2  
Crystal data, data collection parameters and convergence results for the partially racemic solids **1–4**

Compound	<b>1</b>	<b>2</b>	<b>3</b> · H <sub>2</sub> O	<b>4</b>
Empirical formula	C <sub>18</sub> H <sub>25</sub> N <sub>3</sub> O <sub>3</sub> Pd	C <sub>19</sub> H <sub>27</sub> N <sub>3</sub> O <sub>3</sub> Pd	C <sub>19</sub> H <sub>29</sub> N <sub>3</sub> O <sub>3</sub> Pd	C <sub>20</sub> H <sub>29</sub> N <sub>3</sub> O <sub>2</sub> Pd
Formula weight	437.81	451.84	453.85	449.86
Crystal system	Triclinic	Triclinic	Monoclinic	Orthorhombic
Space group	<i>P</i> 1	<i>P</i> 1	<i>C</i> 2	<i>P</i> 2 <sub>1</sub> 2 <sub>1</sub>
<i>a</i> (Å)	8.701(3)	8.9045(8)	10.1063(11)	11.4075(11)
<i>b</i> (Å)	10.816(4)	10.6493(9)	15.4278(16)	16.6662(16)
<i>c</i> (Å)	11.232(4)	10.9999(10)	25.797(3)	20.826(2)
$\alpha$ (°)	74.560(5)	82.406(2)		
$\beta$ (°)	73.631(5)	75.941(2)	98.353(2)	
$\gamma$ (°)	71.615(5)	72.925(2)		
<i>V</i> (Å <sup>3</sup> )	944.0(6)	965.16(15)	3979.5(8)	3959.4(7)
<i>Z</i>	2	2	8	8
<i>D</i> <sub>calc</sub> (g cm <sup>-3</sup> )	1.540	1.555	1.515	1.509
$\mu$ (cm <sup>-1</sup> )	1.004	0.985	0.955	0.956
$\theta$ Range (°)	2.0–30.1	2.5–30.0	0.8–30.0	2.0–30.0
Crystal size (mm <sup>3</sup> )	0.43 × 0.23 × 0.17	0.14 × 0.11 × 0.10	0.44 × 0.26 × 0.07	0.56 × 0.30 × 0.16
Reflections collected	16,008	14,670	18,617	20,940
Reflections unique	9890	10,586	10,958	11,056
<i>R</i> <sub>int</sub>	0.0486	0.0455	0.0472	0.0333
Reflections unique [ <i>I</i> > 2 $\sigma$ ( <i>I</i> )]	8495	8678	10,038	10,106
Variables refined	315	335	473	469
<i>wR</i> <sub>2</sub> (all data)	0.1096	0.0752	0.0715	0.0877
<i>R</i> <sub>1</sub> (all data)	0.0562	0.0621	0.0449	0.0463
<i>R</i> <sub>1</sub> [ <i>I</i> > 2 $\sigma$ ( <i>I</i> )]	0.0473	0.0495	0.0409	0.0410
Goodness-of-fit	1.011	1.005	1.010	1.057
Flack parameter	0.09(4)	−0.02(4)	0.00(3)	−0.01(2)
Resd electron dens max./min. (e Å <sup>-3</sup> )	1.09/−0.95	1.44/−0.85	1.29/−0.72	0.95/−0.55

Table 3  
Crystal data, data collection parameters and convergence results for **5–7**

Compound	<b>5</b>	<b>6</b>	<b>7</b>
Empirical formula	C <sub>18</sub> H <sub>25</sub> N <sub>3</sub> O <sub>3</sub> Pd	C <sub>18</sub> H <sub>25</sub> N <sub>3</sub> O <sub>3</sub> Pd	C <sub>18</sub> H <sub>25</sub> N <sub>3</sub> O <sub>3</sub> Pd
Formula weight	437.81	437.81	437.81
Crystal system	Triclinic	Triclinic	Monoclinic
Space group	<i>P</i> $\bar{1}$	<i>P</i> 1	<i>P</i> 2 <sub>1</sub>
<i>a</i> (Å)	8.6113(9)	8.5200(13)	10.7544(8)
<i>b</i> (Å)	10.9798(11)	10.8331(17)	7.2905(6)
<i>c</i> (Å)	11.1500(11)	11.3749(18)	11.8565(9)
$\alpha$ (°)	73.821(2)	74.315(2)	
$\beta$ (°)	73.510(2)	72.738(2)	98.9460(10)
$\gamma$ (°)	70.693(2)	69.552(2)	
<i>V</i> (Å <sup>3</sup> )	933.92(16)	923.0(2)	918.30(12)
<i>Z</i>	2	2	2
<i>D</i> <sub>calc</sub> (g cm <sup>-3</sup> )	1.557	1.575	1.583
$\mu$ (cm <sup>-1</sup> )	1.015	1.027	1.032
$\theta$ Range (°)	2.0–29.8	2.5–30.0	2.4–30.1
Crystal size (mm <sup>3</sup> )	0.28 × 0.23 × 0.04	0.45 × 0.13 × 0.11	0.30 × 0.20 × 0.14
Reflections collected	13,108	13,625	24,004
Reflections unique	4892	9781	5305
<i>R</i> <sub>int</sub>	0.0555	0.0319	0.0336
Reflections unique [ <i>I</i> > 2 $\sigma$ ( <i>I</i> )]	4065	8205	5236
Variables refined	227	453	227
<i>wR</i> <sub>2</sub> (all data)	0.0813	0.1124	0.0533
<i>R</i> <sub>1</sub> (all data)	0.0544	0.0589	0.0220
<i>R</i> <sub>1</sub> [ <i>I</i> > 2 $\sigma$ ( <i>I</i> )]	0.0413	0.0477	0.0216
Goodness-of-fit	1.037	1.007	1.027
Flack parameter	–	–0.05(3)	0.002(19)
Resd electron dens max./min. (e Å <sup>-3</sup> )	1.46/–0.99	1.44/–0.96	0.59/–0.29

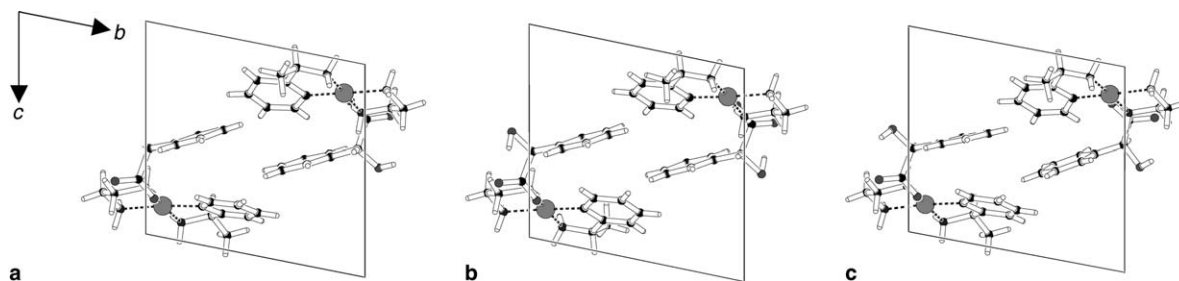


Fig. 5. Unit cell projections of the closely related structures **1** (a), **5** (b) and **6** (c). The structures differ in the relative orientation of the phenyl rings, both in the cations and the anions.

In all three structures **1**, **5**, and **6** the same hydrogen bond pattern is found. One characteristic feature of the resulting two dimensional networks is a  $R_2^2(8)$  motif (Fig. 6(a)) formed by one carboxylate oxygen atom of each anion and an amino group in the chelating en ligand in each of the cations. This structural similarity between the compounds is reflected in their solid state IR spectra in the range between 3400 and 3000 cm<sup>-1</sup>, characteristic for O–H and N–H stretching vibrations. Spectra of **1** and **6**, the two compounds with two symmetrically independent cations and anions, are almost superimposable.

In contrast, **7**, the alternative diastereomeric pair made up from *R* cations and *R* anions, crystallizes in the monoclinic system with an entirely different arrangement of the constituents (Fig. 6(b)). Its smaller volume per formula unit indicates efficient space filling. The structure of **7** is also associated with the highest packing coefficient among

the four compounds sharing the same empirical formula C<sub>18</sub>H<sub>25</sub>N<sub>3</sub>O<sub>3</sub>Pd (Table 4).

A major difference between **7** and the other solids compiled in Table 4 is observed in hydrogen bonding: the maximum number of classical H bonds is formed in the latter compounds, whereas in **7** two donor functionalities, one of the H atoms of each amino group in the cations' en ligand, remain without a suitable partner. For these hydrogen atoms closest distances to potential electronegative acceptors amount to 3 Å. We have performed computer simulations on intermolecular interactions in **1**, **5**, **6** and **7** with the atom-atom potential method; this approach allows to judge relative lattice energies and the relevance of their main contributions, i.e., van der Waals and hydrogen bond energies, to the structures under investigation. The results are summarized in Table 4. Our calculations suggest that total lattice energies as well as their hydrogen bond contribution

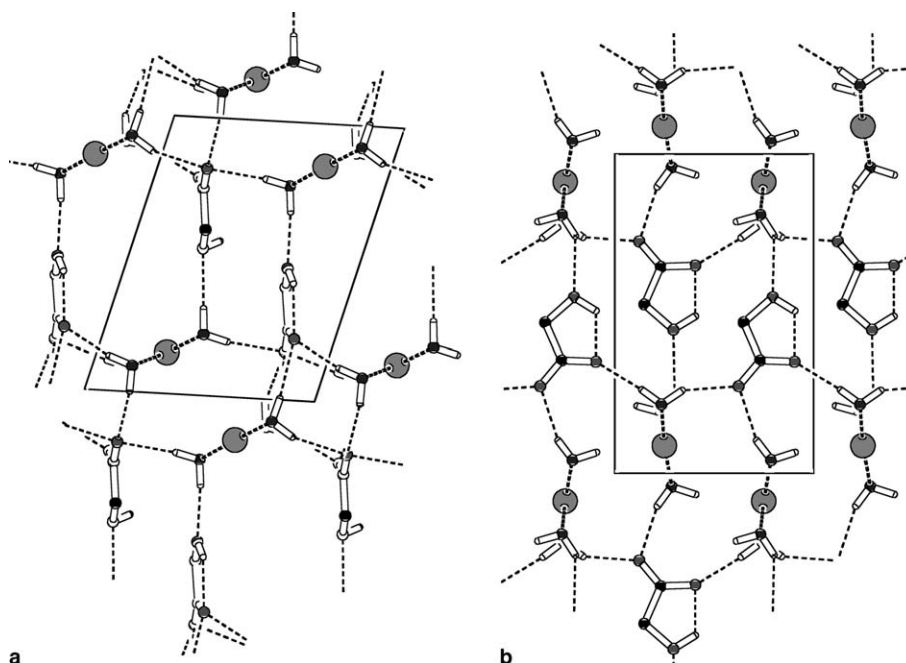


Fig. 6. (a) Hydrogen bond pattern in the structure of **1**; packing is very similar for **5** and **6**, projection is along *c* (the methyl derivative **2** shows a larger unit cell but shares the same packing and H bond pattern). (b) Hydrogen bond pattern in the structure of **7**, projection is along *a*. Only O and N atoms with their hydrogen atoms attached, Pd and the C atoms linking the carboxylate to the hydroxyl group are shown.

Table 4

Space filling properties and lattice energies for **1** and **5–7**, the compounds with empirical formula  $[\text{C}_{10}\text{H}_{18}\text{N}_3\text{Pd}]^+ [\text{C}_8\text{H}_7\text{O}_3]^-$

Compound	<b>1</b>	<b>5</b>	<b>6</b>	<b>7</b>
Crystal system	Triclinic	Triclinic	Triclinic	Monoclinic
Space group	<i>P1</i>	<i>P1</i>	<i>P1</i>	<i>P2<sub>1</sub></i>
<i>V/Z</i> (Å <sup>3</sup> )	472.0(3)	466.96(8)	461.49(12)	459.15(6)
<i>ck</i>	0.696	0.698	0.709	0.718
<i>E/Z</i> (kJ mol <sup>-1</sup> )	-237.0	-236.9	-232.8	-209.0
H bond <i>E/Z</i> (kJ mol <sup>-1</sup> )	-137.8	-137.3	-121.7	-86.2

are very similar for the partially racemic **1** and the fully racemic crystals **5**. One combination of enantiomerically pure cations and anions, namely **6**, also represents a competitive structure in terms of total lattice energy, whereas the alternative diastereomeric salt **7**, is associated with a clearly less favourable total energy. This result concerning the relative energies is corroborated by the experimental finding that **7** shows the best solubility in water. Furthermore, compound **7** is also associated with the lowest decomposition temperature among the cyclopalladated derivatives studied during this work. The lattice energy calculations indicate that the differences between **7** and the other structures are largely due to the inferior contribution of hydrogen bonding interactions in the former compound. When the crystallization alternatives outlined in Scheme 2 are reconsidered and their total lattice energies as compiled in Table 4 are taken into account, the formation of the double salt **1** turns out to be preferred over a macroscopic conglomerate of diastereomeric crystals **6** and **7**.

### 3. Conclusion

We have stated that double salts are probably more frequent than their occurrence in the literature suggests. The question may arise whether our ionic constituents are particularly prone to double salt formation. As for the anions, both mandelic and hydratropic acid are textbook agents for chiral resolution [13]. One might perhaps argue that our cations are “not very chiral” as their enantiomers “only” differ in the orientation of the methyl substituent in the cyclopalladated amine. However, in the organopalladium residues presented in this work as well as in a number of quasiracemic crystals which were synthesized in an entirely different context [27,28] and contain neutral molecules with related ligands, the assignment of chirality was always unambiguous, and the difference between the enantiomers proved sufficient to ensure ordered structures.

After the discussion of our results, it is surely easier to understand the motivation for this study. Considering only the more conventional solids **5**, **6**, and **7**, one might easily draw inappropriate conclusions. Racemic **5** and the combination of *R* configured cations and *S* anions, **6**, are closely related with respect to hydrogen bonding, and their lattice energies are similar. **7** cannot compete with these structures. However, the clearcut difference between the diastereomeric salts **6** and **7** is obviously not sufficient to ensure resolution. The combination of enantiomerically pure cations and a racemic mixture of anions will not simply result in the precipitation of **6**, with compound **7** in solution. In order to obtain the realistic answer “no resolution will be observed”, the partially racemic solid **1** must also be taken

into consideration, either experimentally or via computer simulation. Two problems may arise in the context of the latter approach: First, one may speculate that reality might well be even more complex than the examples we have presented in this study, because our double salts correspond to the most simple 1:1 composition which can be encountered. The hydrate **3** would already be more difficult to deal with than **1** and **2**, and it is easy to imagine more challenging stoichiometries and solvates. Secondly, the calculated energy differences between several of the solids involved may be small (cf. Table 4) and within the accuracy of simple atom–atom potential methods.

## 4. Experimental

### 4.1. General remarks

IR spectra were recorded on a Nicolet Avatar 360 FT IR spectrometer. NMR spectra were measured on a Varian Mercury 200 instrument ( $^1\text{H}$ , 200.0 MHz;  $^{13}\text{C}$ , 50.3 MHz). Chemical shifts are referenced to TMS. Elemental analyses were carried out on a Heraeus CHNO-Rapid apparatus. The thermoanalytical study of **1** was performed with a Mettler-Toledo STAR system with a heating rate of  $10^\circ$  per minute in an atmosphere of dinitrogen.

### 4.2. Preparations

#### 4.2.1. $\text{AgC}_6\text{H}_5\text{CH}(\text{OH})\text{COO}$

Only the preparation of the racemic product is reported; the enantiopure Ag mandelates are synthesized by an analogous procedure.

827 mg (3.0 mmol)  $\text{Ag}_2\text{CO}_3$  are suspended in 150 ml of a mixture  $\text{H}_2\text{O}:\text{CH}_3\text{OH} = 2:1$  at  $60^\circ\text{C}$ . A solution of 913 mg (6.0 mmol) *rac*-mandelic acid in 15 ml  $\text{H}_2\text{O}:\text{CH}_3\text{OH} = 1:2$  at  $60^\circ\text{C}$  is added and the reaction mixture is refluxed for 1.5 h. The hot solution is filtered, and the filtrate is allowed to crystallize overnight at room temperature. Yield 823 mg (53%). Anal. (%) Calc. for  $\text{C}_8\text{H}_7\text{O}_3\text{Ag}$  (found): C, 37.10 (37.01); H, 2.72 (2.88).  $^1\text{H}$  NMR (DMSO- $d_6$ , ppm):  $\delta = 4.79$  (1H, s, broad,  $\text{CH}(\text{OH})$ ), 7.14–7.43 (5H, m, aryl *H*).  $^{13}\text{C}\{^1\text{H}\}$  NMR (DMSO- $d_6$ , ppm):  $\delta = 175.33, 142.68, 127.27, 126.24, 126.10, 73.87$ .

#### 4.2.2. $\text{AgC}_6\text{H}_5\text{CHMeCOO}$

827 mg (3.0 mmol)  $\text{Ag}_2\text{CO}_3$  are suspended in 150 ml of a mixture  $\text{H}_2\text{O}:\text{CH}_3\text{OH} = 2:1$  at  $60^\circ\text{C}$ . A solution of 901 mg (6.0 mmol) *rac*-hydratropic acid in 15 ml  $\text{H}_2\text{O}:\text{CH}_3\text{OH} = 1:2$  at  $60^\circ\text{C}$  is added and the reaction mixture is refluxed for 1.5 h. The hot solution is filtered, and the filtrate is allowed to crystallize overnight at room temperature. Yield 807 mg (52%). Anal. (%) Calc. for  $\text{C}_9\text{H}_9\text{O}_2\text{Ag}$  (found): C, 42.06 (42.06); H, 3.53 (3.79).  $^1\text{H}$  NMR (DMSO- $d_6$ , ppm):  $\delta = 1.34$  (3H, d, 7.1 Hz,  $\text{CH}_3\text{CH}$ ), 3.57 (1H, q, 7.1 Hz,  $\text{CH}_3\text{CH}$ ), 7.14–7.32 (5H, m, aryl *H*).  $^{13}\text{C}\{^1\text{H}\}$  NMR (DMSO- $d_6$ , ppm):  $\delta = 177.27, 143.86, 127.66, 127.22, 125.55, 47.36, 19.91$ .

General comments on the Pd salts: Samples of all compounds but **3** are hygroscopic; their microcrystals or powders become sticky in contact with air, and their CHN analyses consistently indicate the uptake of variable amounts of humidity. CHN analytical data are therefore only reported for **1**, **3** and **7**. Thermal analysis confirmed the presence of ca. 1 mol of water per formula unit in **1** and the decomposition point of  $183^\circ\text{C}$ ; Anal. (%) Calc. for the same batch of **1**,  $\text{C}_{18}\text{H}_{27}\text{N}_3\text{O}_4\text{Pd}$  (found): C, 47.43 (47.60); H, 5.97 (5.73); N, 9.22 (9.70). **3** crystallizes in the form of a stoichiometric monohydrate. Anal. (%) Calc. for  $\text{C}_{19}\text{H}_{29}\text{N}_3\text{O}_3\text{Pd}$  (found): C, 50.28 (50.67); H, 6.44 (6.20); N, 9.26 (9.36). A sufficient quantity of large and stable single crystals was available for **7**; Anal. (%) Calc. for  $\text{C}_{18}\text{H}_{25}\text{N}_3\text{O}_3\text{Pd}$  (found): C, 49.38 (49.20); H, 5.76 (5.72); N, 9.60 (9.33).

Slow evaporation of concentrated solutions represents the simplest technique for growing single crystals appropriate for X-ray diffraction; during this evaporation, formation of metallic palladium is observed. Single crystals of all compounds are colourless and may be handled in air for days without obvious alteration.

Compounds **1–7** do not melt but decompose when heated. The following approximate decomposition temperatures were obtained: **1**,  $183^\circ\text{C}$ ; **2**,  $185^\circ\text{C}$ ; **3**,  $185^\circ\text{C}$ ; **4**,  $185^\circ\text{C}$ ; **5**,  $180^\circ\text{C}$ ; **6**,  $160^\circ\text{C}$ ; **7**,  $145^\circ\text{C}$ .

#### 4.2.3. $[\text{Pd}(\text{C}_6\text{H}_4\text{CHMeNH}_2)(\text{en})]\text{C}_6\text{H}_5\text{CH}(\text{OH})\text{COO}$ , **1**, **5–7**

Only the preparation of **1** (*R* cation, *rac* anion) is reported; **5–7** are synthesized by the same procedure, starting from the appropriate stereoisomers of the components, cf. Scheme 1.

46 mg (0.76 mmol) ethylenediamine are added to a solution of 200 mg (0.38 mmol)  $[\{\text{Pd}(\mu\text{-Cl})(\text{R}-\text{C}_6\text{H}_4\text{CHMeNH}_2)\}_2]$  in 50 ml MeOH at  $50^\circ\text{C}$ . 198 mg (0.76 mmol) *rac*- $\text{AgC}_6\text{H}_5\text{CHOHCOO}$  are added; the suspension is stirred for 30 min and allowed to cool to room temperature, and AgCl is removed by filtration. After evaporation of the solvent in vacuo, the product is obtained in almost quantitative yield.  $^1\text{H}$  NMR (DMSO- $d_6$ , ppm):  $\delta = 1.39$  (3H, d, 6.6 Hz,  $\text{CH}_3\text{CH}$ ), 2.59 (4H, s, broad,  $2\text{CH}_2\text{N}$ ), 3.69 (2H, s, broad, *en*- $\text{NH}_2$ ), 4.13 (1H, m,  $\text{CH}_3\text{CH}$ ), 4.36 (1H, s,  $\text{CHOH}$ ), 4.68 (1H, m,  $\text{NH}_2$ ), 4.77 (2H, s, broad, *en*- $\text{NH}_2$ ), 5.37 (1H, m,  $\text{NH}_2$ ), 6.81–7.37 (9H, m, aryl *H*).  $^{13}\text{C}\{^1\text{H}\}$  NMR (DMSO- $d_6$ , ppm):  $\delta = 173.8, 156.6, 148.7, 144.4, 133.6, 126.9, 126.1, 125.4, 124.2, 123.4, 121.0, 73.5, 58.7, 45.5, 43.3, 24.4$ . The product may be recrystallized from acetonitrile.

**1**, **5**, **6**, and **7** differ in their solid state IR spectra ( $1800\text{--}1000\text{ cm}^{-1}$ , KBr pellets), especially in the region around  $1400\text{ cm}^{-1}$ . Spectra of **1** and **6** are similar.

**1**: 1609s, 1494w, 1456m, 1434w, 1401m, 1373m, 1357m, 1343m, 1284w, 1227w, 1201w, 1172w, 1123w, 1081w, 1054s, 1027w.

**5**: 1607s, 1493w, 1452m, 1399s, 1382m, 1365m, 1283w, 1192w, 1084w, 1053s, 1026m.

**6**: 1609s, 1493w, 1454m, 1434w, 1400s, 1384s, 1359s, 1342m, 1282w, 1226w, 1201w, 1170w, 1109w, 1083w, 1054s, 1026m.

**7**: 1614s, 1495w, 1454m, 1397s, 1384m, 1358s, 1339m, 1292w, 1198m, 1160w, 1115w, 1084w, 1053m, 1032w.

#### 4.2.4. $[Pd(p\text{-MeC}_6\text{H}_3\text{CHMeNH}_2)(en)]\text{C}_6\text{H}_5\text{CHOHCOO}$ , **2**

46 mg (0.76 mmol) ethylenediamine are added to a solution of 210 mg (0.38 mmol)  $[\{Pd(\mu\text{-Cl})(R\text{-MeC}_6\text{H}_3\text{CHMeNH}_2)\}_2]$  in 50 ml MeOH at 50 °C. 198 mg (0.76 mmol) *rac*- $\text{AgC}_6\text{H}_5\text{CHOHCOO}$  are added; the suspension is stirred for 30 min and allowed to cool to room temperature, and AgCl is removed by filtration. After evaporation of the solvent in vacuo, the product is obtained in almost quantitative yield.  $^1\text{H}$  NMR (DMSO- $d_6$ , ppm):  $\delta$  = 1.35 (3H, d, 6.4 Hz,  $\text{CH}_3\text{CH}$ ), 2.16 (3H, s, aryl- $\text{CH}_3$ ), 2.59 (4H, m, broad,  $2\text{CH}_2\text{N}$ ), 3.70 (2H, s, broad, en- $\text{NH}_2$ ), 4.08 (1H, m,  $\text{CH}_3\text{CH}$ ), 4.48 (1H, s,  $\text{CHOH}$ ), 4.69 (1H, m,  $\text{NH}_2$ ), 4.76 (2H, s, broad, en- $\text{NH}_2$ ), 5.36 (1H, m,  $\text{NH}_2$ ), 6.71–7.39 (8H, m, aryl *H*).  $^{13}\text{C}\{^1\text{H}\}$  NMR (DMSO- $d_6$ , ppm):  $\delta$  = 173.9, 153.7, 148.1, 144.0, 134.2, 132.6, 127.1, 126.1, 125.7, 124.1, 120.8, 73.6, 58.4, 45.5, 43.3, 24.4, 20.9. The product may be recrystallized from acetonitrile.

#### 4.2.5. $[Pd(\text{C}_6\text{H}_4\text{CHMeNH}_2)(en)]\text{C}_6\text{H}_5\text{CHMeCOO}$ , **3**

46 mg (0.76 mmol) ethylenediamine are added to a solution of 200 mg (0.38 mmol)  $[\{Pd(\mu\text{-Cl})(R\text{-C}_6\text{H}_4\text{CHMeNH}_2)\}_2]$  in 50 ml MeOH at 50 °C. 196 mg (0.76 mmol) *rac*- $\text{AgC}_6\text{H}_5\text{CHMeCOO}$  are added; the suspension is stirred for 30 min and allowed to cool to room temperature, and AgCl is removed by filtration. After evaporation of the solvent in vacuo, the product is obtained in almost quantitative yield as a monohydrate **3** ·  $\text{H}_2\text{O}$ .  $^1\text{H}$  NMR (DMSO- $d_6$ , ppm):  $\delta$  = 1.22 (3H, d, 7.1 Hz,  $\text{CH}_3\text{CH}$  cation), 1.34 (3H, d, 6.6 Hz,  $\text{CH}_3\text{CH}$  anion), 2.55 (4H, m, broad,  $2\text{CH}_2\text{N}$ ), 3.23 (1H, q, 7.1 Hz,  $\text{CH}_3\text{CH}$  anion), 4.05 (2H, s, broad, en- $\text{NH}_2$ ), 4.15 (1H, m,  $\text{CH}_3\text{CH}$  cation), 4.76 (2H, s, broad, en- $\text{NH}_2$ ), 5.11 (1H, m,  $\text{NH}_2$ ), 5.71 (1H, m,  $\text{NH}_2$ ), 6.74–7.29 (9H, m, aryl *H*).  $^{13}\text{C}\{^1\text{H}\}$  NMR (DMSO- $d_6$ , ppm):  $\delta$  = 175.9, 157.2, 149.4, 146.3, 133.8, 127.4, 127.3, 124.7, 124.1, 123.3, 121.0, 58.6, 49.4, 45.8, 43.2, 24.3, 20.4. The product may be recrystallized from methanol or methanol/water mixtures.

#### 4.2.6. $[Pd(p\text{-MeC}_6\text{H}_3\text{CHMeNH}_2)(en)]\text{C}_6\text{H}_5\text{CHMeCOO}$ , **4**

46 mg (0.76 mmol) ethylenediamine are added to a solution of 210 mg (0.38 mmol)  $[\{Pd(\mu\text{-Cl})(R\text{-MeC}_6\text{H}_3\text{CHMeNH}_2)\}_2]$  in 50 ml MeOH at 50 °C. 196 mg (0.76 mmol) *rac*- $\text{AgC}_6\text{H}_5\text{CHMeCOO}$  are added; the suspension is stirred for 30 min and allowed to cool to room temperature, and AgCl is removed by filtration. After evaporation of the solvent in vacuo, the product is obtained in almost quantitative yield.  $^1\text{H}$  NMR (DMSO- $d_6$ , ppm):  $\delta$  = 1.25 (3H, d, 7.1 Hz,  $\text{CH}_3\text{CH}$  cation), 1.34 (3H, d, 6.6 Hz,

$\text{CH}_3\text{CH}$  anion), 2.16 (3H, s, aryl- $\text{CH}_3$ ), 2.56 (4H, m, broad,  $2\text{CH}_2\text{N}$ ), 3.31 (1H, q, 7.1 Hz,  $\text{CH}_3\text{CH}$  anion), 3.87 (2H, s, broad, en- $\text{NH}_2$ ), 4.05 (1H, m,  $\text{CH}_3\text{CH}$  cation), 4.75 (2H, s, broad, en- $\text{NH}_2$ ), 4.82 (1H, m,  $\text{NH}_2$ ), 5.50 (1H, m,  $\text{NH}_2$ ), 6.70–7.29 (8H, m, aryl *H*).  $^{13}\text{C}\{^1\text{H}\}$  NMR (DMSO- $d_6$ , ppm):  $\delta$  = 176.4, 153.9, 148.6, 145.6, 134.3, 132.5, 127.4, 127.3, 124.9, 124.0, 120.7, 58.3, 48.5, 45.6, 43.2, 24.3, 20.9, 20.3. The product may be recrystallized from acetonitrile.

### 4.3. Lattice energy minimizations

Local energy minima for the crystal structures of **1**, **5**, **6**, and **7** were obtained using the program PCK83 [29]. Prior to minimization experimental distances to H atoms were normalized to the following values: C–H 1.083, N–H 1.009, O–H 0.983 Å. Independent residues were treated as rigid objects in their experimentally observed conformation and were allowed to translate and rotate. Van-der-Waals interactions were simulated with a Buckingham potential using published parameters [30]. The intermolecular N–H···O hydrogen bonds were modelled by an additional attractive exponential function of the type  $E = -8184.5 \times \exp(-2.9 \times r_{ij})$  ( $E$  in  $\text{kJ mol}^{-1}$ ,  $r_{ij}$  in Å).

### 4.4. Single crystal X-ray diffraction

Intensity data were collected on a Bruker-Nonius D8 goniometer equipped with an APEX CCD area detector at 110 K with Mo  $\text{K}\alpha$  radiation (graphite monochromator,  $\lambda = 0.71073$  Å).

Empirical absorption corrections were performed with SADABS [31]. The structures were solved by direct methods [32] and refined on  $F^2$  [33]. Tables 2 and 3 compile crystal data, data collection parameters and convergence results.

Packing coefficients were calculated with the help of the program PLATON [22].

## 5. Supplementary material

Results of the single crystal X-ray diffraction experiments on **1**–**7** have been deposited in CIF format at the Cambridge Crystallographic Data Centre, CCDC, Nos. 285389 (**1**), 285390 (**2**), 285391 (**3** ·  $\text{H}_2\text{O}$ ), 285392 (**4**), 285393 (**5**), 285394 (**6**), and 285395 (**7**). Copies of the data can be obtained free of charge on application to The Director, CCDC, 12 Union Road, Cambridge, CB2 1EZ, UK, fax: +44 1223 366 033, e-mail: deposit@ccdc.ac.uk or on the web www: <http://www.ccdc.cam.ac.uk>.

### Acknowledgements

This work was supported by Deutsche Forschungsgemeinschaft (“Racemic Crystals and Conglomerates”). The authors thank BASF for providing the enantiomerically pure primary amines.

## References

- [1] E.L. Eliel, S.H. Wilen, *Stereochemistry of Organic Compounds*, Wiley, New York, 1993.
- [2] W.J. Pope, *J. Chem. Soc.* 97 (1910) 987.
- [3] A. Ladenburg, *Liebigs Ann. Chem.* 364 (1908) 227.
- [4] M. Delépine, F. Larèze, *Bull. Soc. Chim. Fr.* 104 (1955) 104.
- [5] H. Okazaki, U. Sakaguchi, H. Yoneda, *Inorg. Chem.* 22 (1983) 1539.
- [6] M. Gajhede, S. Larsen, *Acta Crystallogr. Sect. B* 42 (1986) 172.
- [7] T. Mizuta, K. Toshitani, K. Miyoshi, H. Yoneda, *Inorg. Chem.* 29 (1990) 3020.
- [8] T. Mizuta, K. Toshitani, K. Miyoshi, *Bull. Chem. Soc. Jpn.* 64 (1991) 1183.
- [9] S. Larsen, H. Lopez de Diego, D. Kozma, *Acta Crystallogr. Sect. B* 49 (1993) 310.
- [10] K. Kinbara, K. Sakai, Y. Hashimoto, H. Nohira, K. Saigo, *J. Chem. Soc., Perkin Trans. 2* (1996) 2615.
- [11] S.-G. Kim, K.-H. Kim, Y.K. Kim, S.K. Shin, K.H. Ahn, *J. Am. Chem. Soc.* 125 (2003) 13819.
- [12] K. Kinbara, K. Saigo, in: S.E. Denmark (Ed.), *Topics in Stereochemistry*, vol. 23, Wiley, New York, 2003, p. 207.
- [13] J. Jacques, A. Collet, S.H. Wilen, *Enantiomers, Racemates, and Resolutions*, Krieger Publishing Company, Malabar, FL, 1994, a list of “putative double salts” is given on page 296.
- [14] H. Lopez de Diego, *Acta Crystallogr. Sect. C* 50 (1994) 1995.
- [15] O.M. Peeters, N.M. Blaton, C.J. De Ranter, *Acta Crystallogr. Sect. C* 53 (1997) 597.
- [16] J. Vicente, I. Saura-Llamas, M.G. Palin, *Organometallics* 16 (1997) 826.
- [17] Y. Fuchita, K. Yoshinaga, Y. Ikeda, J. Kinoshita-Kawashima, *J. Chem. Soc., Dalton Trans.* (1997) 2495.
- [18] P.H. Leung, A.C. Willis, S.B. Wild, *Inorg. Chem.* 31 (1992) 1406.
- [19] S.Y.M. Chooi, T.S.A. Hor, P.H. Leung, K.F. Mok, *Inorg. Chem.* 31 (1992) 1494.
- [20] S.Y.M. Chooi, S.-Y. Siah, P.H. Leung, K.F. Mok, *Inorg. Chem.* 32 (1993) 4812.
- [21] J. Albert, R. Bosque, J.M. Cadena, S. Delgado, J. Granell, *J. Organomet. Chem.* 634 (2001) 83.
- [22] A.L. Spek, *J. Appl. Cryst.* 36 (2003) 7.
- [23] M.C. Etter, J.C. MacDonald, J. Bernstein, *Acta Crystallogr. Sect. B* 46 (1990) 256.
- [24] J. Grell, J. Bernstein, G. Tinhofer, *Acta Crystallogr. Sect. B* 55 (1999) 1030.
- [25] S. Larsen, H. Lopez de Diego, *Acta Crystallogr. Sect. B* 49 (1993) 303.
- [26] We can neither exclude nor predict the existence of structures with a more complicated stoichiometry under certain crystallization conditions; we have published an example for a 1:3 quasiracemic crystal based on neutral molecules: U. Englert, A. Häring, C. Hu, I. Kalf, *Z. Anorg. Allg. Chem.* 628 (2002) 1173.
- [27] B. Calmuschi, M. Alesi, U. Englert, *Dalton Trans.* (2004) 1852.
- [28] B. Calmuschi, U. Englert, *CrystEngComm* 7 (2005) 171.
- [29] D.E. Williams, *PCK83*, A Crystal Molecular Packing Analysis Program, Quantum Chemistry Programs Exchange, 1983.
- [30] U. Englert, in: M. Hargittai, I. Hargittai (Eds.), *Advances in Molecular Structure Research*, vol. 6, JAI Press Inc., Greenwich, Connecticut, 2000, p. 49.
- [31] G.M. Sheldrick, *SADABS*, Program for Empirical Absorption Correction of Area Detector Data, University of Göttingen, 1996.
- [32] G.M. Sheldrick, *SHELXS97*, Program for Crystal Structure Solution, University of Göttingen, 1997.
- [33] G.M. Sheldrick, *SHELXL97*, Program for Crystal Structure Refinement, University of Göttingen, 1997.